Theoretical model of homogeneous metal–insulator–metal perfect multi-band absorbers for the visible spectrum

You may also be interested in:

Ultra-compact metamaterial absorber for multiband light absorption at mid-infrared frequencies
Dong Xiao and Keyu Tao

Flexible metamaterial absorbers with multi-band infrared response
Govind Dayal and S Anantha Ramakrishna

Tri-layered composite plasmonic structure with a nanohole array for multiband enhanced absorption at visible to NIR frequencies: plasmonic and metamaterial resonances
Gangadhar Behera and S Anantha Ramakrishna

Polarization-insensitive and wide-angle broadband nearly perfect absorber by tunable planar metamaterials in the visible regime
Xiaoyang Duan, Shuqi Chen, Wenwei Liu et al.

Metal–insulator–metal light absorber: a continuous structure
M Yan

Design of periodic metal-insulator-metal waveguide back structures for the enhancement of light absorption in thin-film solar cells
Zheng Gai-Ge, Jiang Jian-Li, Xian Feng-Lin et al.

Nanostructure arrays in free-space: optical properties and applications
Stéphane Collin

Design of multi-band metamaterial perfect absorbers with stacked metal–dielectric disks
Govind Dayal and S Anantha Ramakrishna

Theoretical model of homogeneous metal–insulator–metal perfect multi-band absorbers for the visible spectrum

G Kajtár[1], **M Kafesaki**[1,2], **E N Economou**[1,3] **and C M Soukoulis**[1,4]

[1] Institute of Electronic Structure and Laser, Foundation for Research and Technology–Hellas, 70013 Heraklion, Greece
[2] Department of Materials Science and Technology, University of Crete, 71003 Heraklion, Greece
[3] Physics Department, University of Crete, 71003 Heraklion, Greece
[4] Ames Lab and Department of Physics and Astronomy, Iowa State University, Ames, Iowa 50011, USA

E-mail: gergely@iesl.forth.gr

Abstract

We present a rigorous study of the perfect absorption properties of metal–insulator–metal (MIM) structures in the visible spectrum. We provide a derivation (based on the transfer matrix method) and analysis of the conditions for which the perfect absorption occurs. We show that these conditions are fulfilled when the incident wave excites the eigenmodes of the structure. The quantitative analysis allows us to design specific perfect absorbers for our needs. The analytical model is verified by rigorous simulations based on rigorous coupled wave analysis, which demonstrate also the angle and polarization insensitivity of the absorption properties of such a structure. Employing the MIM approach and results, we also investigate and demonstrate multiple perfect absorption bands and broad-band absorption in properly designed multilayer metal-insulator systems.

Keywords: thin films, perfect absorbers, photonics

(Some figures may appear in colour only in the online journal)

1. Introduction

Nanostructured photonic devices involving metallic components enable to control and manipulate the light at subwavelength scales, thus exhibiting unique optical properties and functionalities, such as extraordinary transmission, high field concentration and confinement, subwavelength guiding etc. One important such a functionality, strongly related to high field concentration and confinement, is perfect absorption. Perfect absorption can find unique possibilities in a variety of research and application areas, including photovoltaics and thermophotovoltaics, light emitting diodes, electromagnetic shielding devices, etc [1, 2]. However, one of the most commonly encountered problem of today's high absorption systems is their sensitivity to polarization and/or angle of incidence of the impinging radiation. Usually the perfect absorption is preserved only for a small incidence angle range or for a given polarization [3, 4]. Moreover, most of the absorbers

discussed in the literature are quite narrow-band, as a result of the resonance origin of the high absorption [5–8].

Here we demonstrate and analyze theoretically and numerically a perfectly absorbing yet simple metal–insulator–metal (MIM) sandwiched structure which avoids the above mentioned angle and polarization restrictions, while it can be easily extended to give multi-band and broad-band absorption.

MIM based absorbers with a structured top metallic layer have been widely studied [9–15][5]. The structured (in 1D or

[5] Metal Insulator Metal (MIM) structures with oxide as the insulating material are extensively used as diodes, exploiting the electron tunneling through the very thin (of few nm) oxide layer. The aim and operation principle/conditions of such systems are different from the MIM electromagnetic absorbers discussed in this work, where the electromagnetic rather than the electronic response/properties is the issue under investigation (here the dielectric layer thickness is much larger than just few nm). For example MIM absorbers as the ones presented here are not very sensitive to small (of the order of nm) dielectric-layer thickness variations (resulting, e.g. from temperature variation during fabrication), as the electronic tunneling diodes.
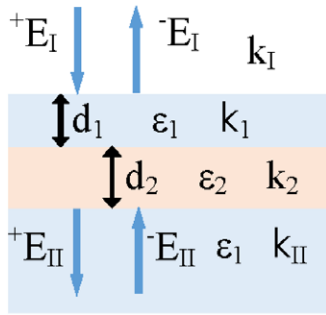
Figure 1. Scheme of the two layer system embedded in metallic substrate and air superstrate. The top layer (of thickness d_1) and the substrate have the same relative permittivity ε_1. The middle dielectric layer has relative permittivity ε_2 and thickness d_2. k_1 and k_2 denote the wavenumbers in the corresponding layers; for the rest of the symbols see text describing equation (1).

2D) top metal layers of such absorbers can either (a) possess localized surface plasmon resonances at near-infrared or visible spectra, which enhance the nearby field and result to high losses in both metallic nanostructures and the subsequent dielectric/absorbing layer, or (b) enhance the coupling of the incident radiation with the guided (cavity) modes of the dielectric/absorbing layer, or (c) couple resonantly with the bottom metallic layer in such a way which leads to high field concentration in the intermediate dielectric layer (e.g. magnetic resonance coupling) leading to high absorption. Nanostructured MIM absorbers require for their fabrication lithographic techniques, e.g. e-beam lithography or nanoimprint lithography, which implies high fabrication cost and time, limiting thus the total fabrication area. The proposed here MIM absorber consists of homogeneous, non-structured layers (see figure 1), avoiding all the fabrication complications of nanostructured top-layer absorbers and ensuring isotropic and polarization insensitive response, as well as easily achievable multiband and broadband operation.

Although such MIM structures have been analytically investigated extensively so far, their investigation as electromagnetic wave manipulation systems concerned mainly their exploitation as guiding devices [15], or color filters [16] and less as absorbers, while a rigorous analytical study and derivation of the perfect absorption conditions is still lacking, leaving also the rigorous theoretical background unexploited. While many papers focus on the infrared spectrum [17–20], in this paper we analytically investigate and derive the conditions for the perfect absorption in MIM systems for the visible spectrum. Exploiting these conditions we demonstrate nearly 100% absorption in properly designed MIM structures made of silver as the metal and microcrystalline silicon as the dielectric absorbing material. The choice of microcrystalline silicon is dictated by its wide use in today's thin film solar cells, which comprise one of the most desired paths for the perfect absorption exploitation. (An alternative dielectric material would be amorphous silicon which has though similar optical properties as microcrystalline silicon.)

The high absorption demonstrated here is highly insensitive to incident wave polarization and survives even for large incidence angles. Moreover, exploiting further this MIM absorber approach we propose a multilayer MIM system able to provide multiple-band and broad-band absorption. Specifically, the rest of the paper is organized as follows:

In section 2 we present a rigorous analytic derivation of the total absorption conditions in MIM systems. We show that the total absorption occurs when the incident wave excites an eigenmode of the middle dielectric layer, which serves as a Fabry–Perot cavity. Conditions for these excitations are derived. In section 3 we verify our theoretical analysis with Rigorous Coupled Wave Analysis (RCWA—[21]) calculations for a specific silver-microcrystalline silicon-silver MIM structure. The structure is designed to have its absorption peak in the optical spectral regime. Section 4 contains the description of a multi-layered MIM sandwich structure featuring multiple high absorption bands.

2. Theoretical model

In this section we introduce a transfer matrix description of a two layered system embedded in two semi-infinite media (metallic substrate and air superstrate). Altough a MIM structure has three layers, this two layered model can actually represent a three layered MIM structure, since the bottom metallic layer of a MIM structure is usually thick enough to mimic a semi-infinite metallic substrate, causing nearly zero transmitted energy. We consider the relative permeability everywhere to be equal to 1. The metallic media (top layer and semi-infinite substrate) have relative permittivity ε_1 with negative real part and zero imaginary part (for the simplicity of analytical derivation), the middle dielectric layer has relative permittivity ε_2 with positive real part and small non-zero imaginary part. The metallic top layer and the dielectric middle layer have thickness d_1 and d_2, respectively (see figure 1). Normal incidence is considered. The transfer matrix $\mathbf{M}$ relates the inbound ($^-E_{II}$) and outbound ($^+E_{II}$) electric field amplitudes in the substrate with the inbound (^+E_I) and outbound (^-E_I) electric field amplitudes in the superstrate [23]:

$$\begin{pmatrix} ^-E_I \\ ^+E_I \end{pmatrix} = \mathbf{M} \begin{pmatrix} ^-E_{II} \\ ^+E_{II} \end{pmatrix} = \begin{pmatrix} \mathbf{M}_{11} & \mathbf{M}_{12} \\ \mathbf{M}_{21} & \mathbf{M}_{22} \end{pmatrix} \begin{pmatrix} ^-E_{II} \\ ^+E_{II} \end{pmatrix}. \tag{1}$$

Since the wave in the substrate is evanescent, total absorption occurs when the reflected wave is zero, i.e. $^-E_I = 0$. We consider here no incident wave in the substrate ($^-E_{II} = 0$). The zero reflection condition in this case is fulfilled if $\mathbf{M}_{12} = 0$ (see equation (1)). The transfer matrix $\mathbf{M}$ for the given structure is defined as $\mathbf{M} = \mathbf{S}_I \mathbf{S}_1 \mathbf{S}_2 \mathbf{S}_{II}$, where matrices $\mathbf{S}$ stand for each region: the superstrate, the top metallic layer, the middle dielectric layer and the substrate, respectively. These matrices are derived from Maxwell equations and have the following forms [23]:

$$\mathbf{S}_I = \begin{pmatrix} 1 & 1 \\ k_I & -k_I \end{pmatrix}^{-1} \tag{2}$$

$$\mathbf{S}_{II} = \begin{pmatrix} 0 & e^{ik_{II}(d_1+d_2)} \\ 0 & -k_{II}e^{ik_{II}(d_1+d_2)} \end{pmatrix}. \tag{3}$$

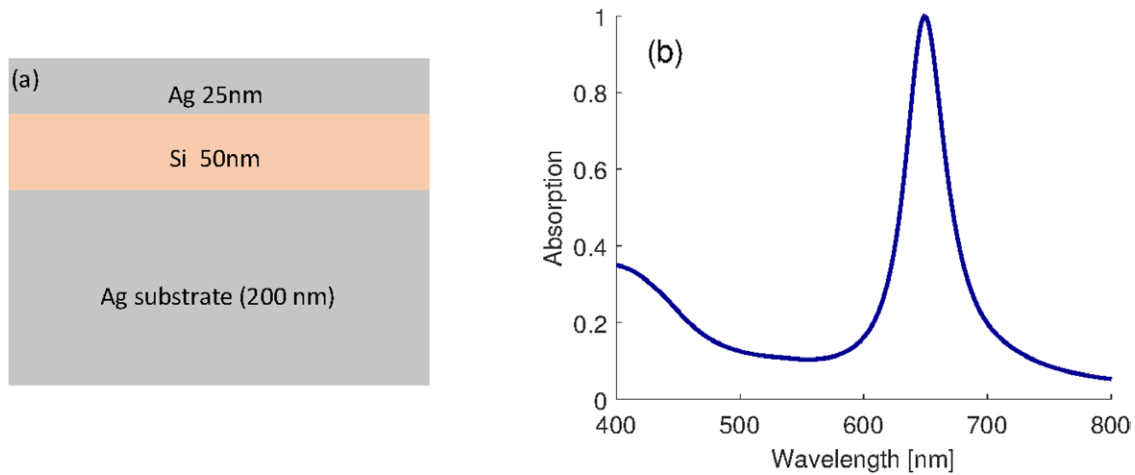J. Phys. D: Appl. Phys. **49** (2016) 055104

G Kajtár *et al*

Figure 2. (a) The structure of a MIM perfect absorber. (b) Numerically obtained (through RCWA) absorption spectrum showing perfect absorption at 649 nm wavelength for the structure of panel (a).

Matrices $\mathbf{S}_1$ and $\mathbf{S}_2$ in general form read as

$$\mathbf{S}_j = \begin{pmatrix} \cos(k_j d_j) & \frac{i}{k_j}\sin(k_j d_j) \\ i k_j \sin(k_j d_j) & \cos(k_j d_j) \end{pmatrix}, \quad j = 1, 2. \tag{4}$$

Here, $k_{\mathrm{I}} = k = \omega/c$ is the wavenumber in vacuum, for a wave of angular frequency ω (c is the vacuum light velocity). Inside the top metallic layer and the substrate the waves are evanescent, so the wavenumbers are purely imaginary, i.e. $k_1 = k_{\mathrm{II}} = ik\sqrt{-\varepsilon_1}$ (note that ε_1 has been considered with zero imaginary part). Inside the dielectrics the wavenumber is $k_2 = k\sqrt{\varepsilon_2}$. By substituting equations (2)–(4) to equation (1), we calculate the condition for the resonant wavelength inside the dielectric layer as

$$\cot(\sqrt{\varepsilon_2}\, d_2 k) = \frac{1}{2}\left(\sqrt{-\frac{\varepsilon_2}{\varepsilon_1}} - \sqrt{-\frac{\varepsilon_1}{\varepsilon_2}} \right). \tag{5}$$

Incidentally, the solutions of equation (5) also represent the guided modes of a dielectric slab with relative permittivity ε_2 and thickness d_2 embedded in a medium with relative permittivity ε_1 in a general form [23]. These bound states normally cannot be excited from the outside. The top metallic layer has the role to bound the incident wave to the dielectric layer by the evanscent wave propagating through the top metallic layer. The perfect absorption condition obtained from transfer matrix (requiring $\mathbf{M}_{12} = 0$) then results to the condition for the top metallic layer thickness:

$$\tanh(\sqrt{-\varepsilon_1}\, d_1 k) = \frac{\sqrt{-\frac{\varepsilon_1}{\varepsilon_2}}\tan(\sqrt{\varepsilon_2}\, d_2 k) + 1}{\sqrt{-\frac{\varepsilon_2}{\varepsilon_1}}\tan(\sqrt{\varepsilon_2}\, d_2 k) - 1}. \tag{6}$$

If equations (5)–(6) are fulfilled, the incident wave tunnels through the top metallic layer, excites the eigenmode of the cavity and is perfectly absorbed there. Please note that the derivation for TM-polarized wave leads to the same result because of the normal incidence.

3. Perfect metal–insulator–metal absorber

In this section we numerically calculate the absorption of a realistic MIM structure and compare the results with the analytical model presented in the previous section. The MIM structure consists of a silver substrate with 200 nm thickness and a top silver layer with 25 nm thickness (figure 2(a)). The silver's relative permittivity is obtained from [24]. Between the silver layers, in the middle, there is a 50 nm thick dielectric layer made of microcrystalline silicon with relative permittivity given in [25] (the silicon permittivity in the wavelength ranging from 400–800 nm). Numerical calculations of the absorption, obtained using the RCWA method [21][6], show that the perfect absorption occurs for 649 nm wavelength (see figure 2(b)) for the normal incidence. According to the theoretical model presented in the previous section, such a structure has perfect absorption at 630 nm (equation (5)) with 35 nm silver top layer (equation (6)). The difference is caused by the realistic material model used in the rigorous calculation, which involves non-zero absorption of the silver, hence in the theoretical model the top metallic layer is not absorbing. Furthermore, the theoretical model assumes that the imaginary part of the dielectric permittivity is negligible compared to the real part, which is not always the case in the realistic systems.

In order to test the theory further, we numerically obtain for every free-space-wavelength in the (400, 800) nm interval and every dielectric layer thickness in the (0, 250) nm interval the required top silver layer thickness for which the absorption is higher than 95%. The results, which have been obtained by our own home-made code based on the RCWA[7], are shown

---

[6] Our home-made tool employed in the simulations presented here is available at http://rawdogapp.weebly.com/. A detailed description of this tool and comparison with the commercial software RSoft are available in the dissertation thesis by Kajtar: 'Electromagnetic properties of double-periodic structures', which can be downloaded from http://rawdogapp.weebly.com/uploads/2/3/1/9/23191398/dissertation_thesis.pdf. The tool is based on the Rigorous Coupled Wave Analysis (RCWA) method which solves the steady-state Maxwell's equations transforming them into the Fourier space. A thorough presentation of the method can be be also found in [21].

[7] See footnote 6.

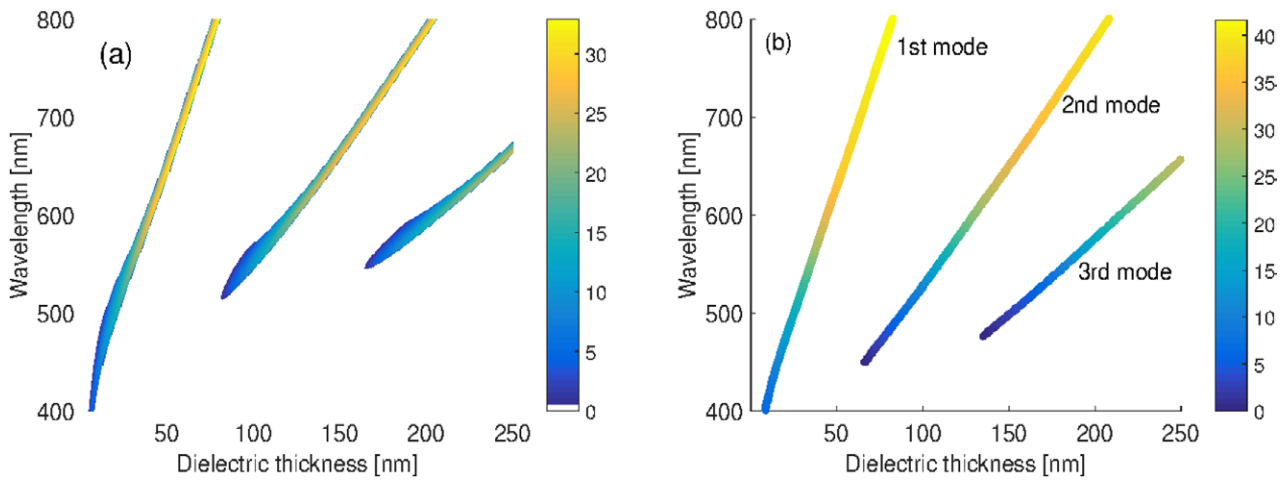J. Phys. D: Appl. Phys. **49** (2016) 055104

G Kajtár *et al*

Figure 3. (a) RCWA simulation showing the regions in the plane, thickness of dielectric layer versus wavelength, corresponding to absorption higher than 95%; the color code in these regions (in connection with the vertical bar) indicates the thickness of the upper metallic layer (in nanometers) necessary for achieving this level of absorption. (b) The same as in panel (a), calculated analytically from equations (5)–(6).
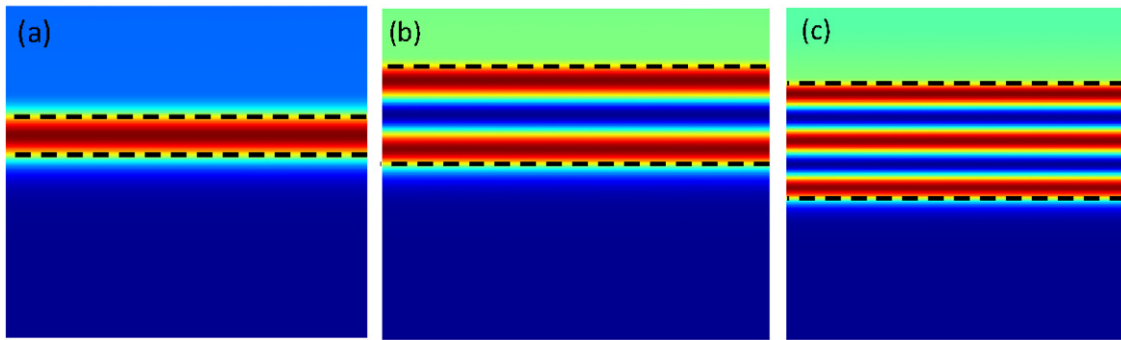

Figure 4. Electric field intensity distribution of different MIM structures when the perfect absorption occurs for different modes at wavelength 630 nm. (a) First mode for dielectric layer thickness 46 nm. (b) Second mode for dielectric layer thickness 135 nm. (c) Third mode for dielectric layer thickness 225 nm. Black dashed lines indicate the boundaries of the dielectric cavity.
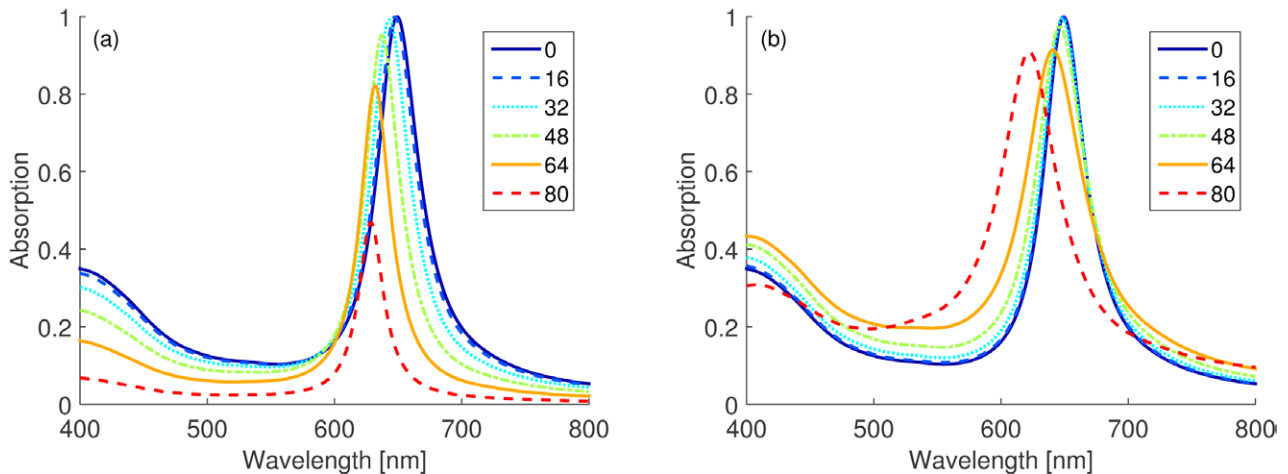

Figure 5. Absorption spectra for TE (a) and TM (b) polarized incident wave for the structure of figure 2(a) for various angles of incidence, indicated in the legends.

in figure 3(a). Apparently, there are three different modes present for the given wavelength interval. These modes correspond to the first three solutions of equation (5). The analytically calculated wavelengths (obtained using equation (5)) for these modes, as a function of silicon thickness, are plotted in figure 3(b), revealing an excellent agreement with the accurate numerical data. From these results we conclude that thicker dielectric absorbers require thicker top metallic layer to trap the incident light inside the dielectric cavity, trapping of course longer wavelengths.

Figure 4 shows the field intensity distribution inside the dielectric cavity when the perfect absorption occurs for the three
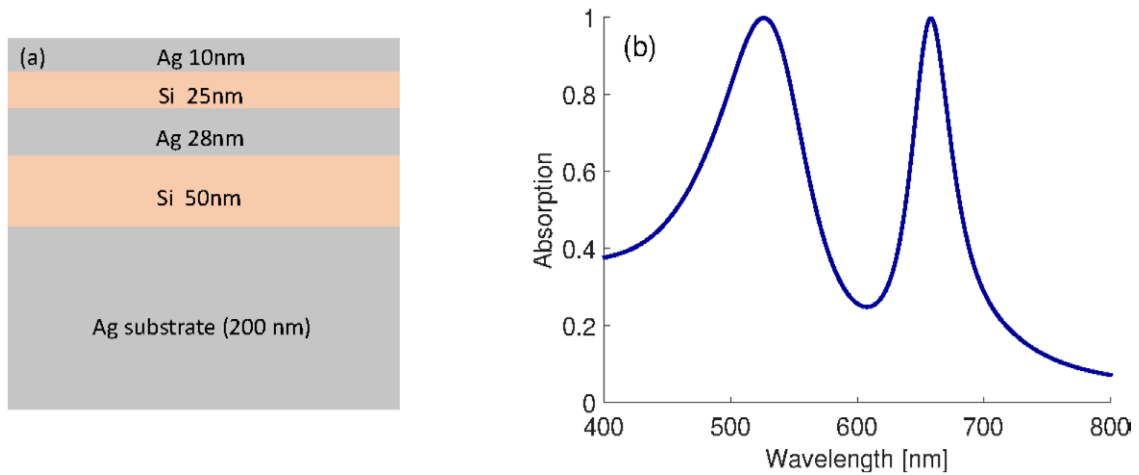
J. Phys. D: Appl. Phys. **49** (2016) 055104

G Kajtár *et al*

Figure 6. (a) Scheme of the double MIM structure with with respective thicknesses. (b) The absorption spectrum for the structure of panel (a) possesses two maxima, at wavelengths 526 nm and 658 nm, respectively. Normal incidence.
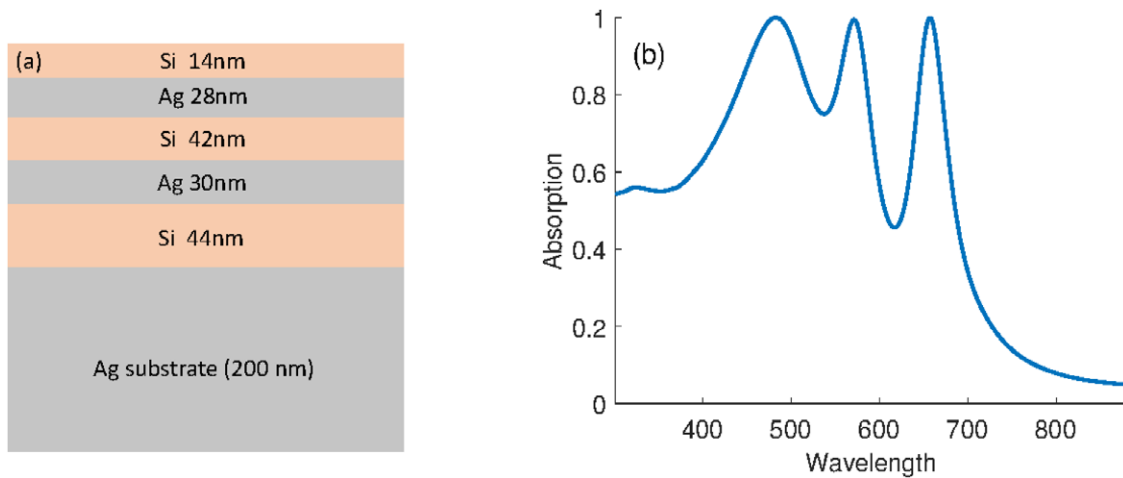

Figure 7. (a) Scheme of the MIM structure with three dielectric layers with the respective thicknesses. (b) The absorption spectrum for the structure of panel (a) possesses three overlapping high absorption bands. Normal incidence has been considered.

different modes. Evidently, the energy is concentrated inside the cavity. Field visualisation was made by JCMwave software[8].

Undoubtedly, for a structure to be characterized as a perfect absorber, the high absorption should be maintained also for oblique incidence and any incident wave polarization. To examine the absorption response of our structure for off-normal incidence, absorption spectra for different angles of incidence (0°, 18°, 32°, 48°, 64°, 80°) are calculated for TE—the electric field vector is parallel to the surface—(figure 5(a)) and TM—the magnetic field vector is parallel to the surface—(figure 5(b)) polarized incident waves, for the structure of figure 2(a). As it can be seen in figure 5, high absorption is observable even for large angles of incidence, especially for the TM polarized wave, where the maximum absorption is near 90% for even 80° angle of incidence.

4. Multi-layered perfect absorbers

Prompted by the conclusion of the previous section that thicker dielectric layers, which absorb longer wavelengths, require

[8] www.jcmwave.com

thicker top metallic layers to trap the wave, we examined the possibility to use multilayer MIM structures to achieve multiband perfect absorption, with ultimate aim to realize a broadband perfect absorber. In this section we show that such a realization is indeed possible. Properly designed multilayered MIM structures possess multiple perfect absorption bands. If the structure consists of two dielectric layers made of microcrystalline silicon sandwiched between silver layers (see figure 6(a)), the incident wave can induce resonant modes independently inside each dielectric cavity. The longer resonant wavelength penetrates the second metallic layer and couples with the first eigenmode of the thicker cavity. The shorter resonant wavelength couples with the first eigenmode of the first dielectric cavity. Each wavelength excites its respective cavity. This works independently for each wavelength-cavity pair. The materials of this structure are the same, i.e. silver and silicon, as in the previous section. The thicknesses of the layers from top to bottom are as follows: 10 nm (Ag), 25 nm (Si), 28 nm (Ag), 50 nm (Si). The silver substrate has to be thick enough to mimic a semi-infinite medium (in our simulations 200 nm). The numerically calculated absorption spectrum is plotted in figure 6(b).

Adding another dielectric layer to the top of the previous structure enables the design of a structure with three high absorption peaks. Figure 7(a) shows the scheme of the simulated structure. The three high absorption peaks occur at wavelengths 482 nm, 571 nm and 656 nm, respectively, as shown in figure 7(b). The results of figure 7(b), which show high absorption spanning almost the entire visible spectrum, demonstrate the possibility of realization of broadband and polarization and angle insensitive perfect absorbers applying MIM design.

5. Conclusions

In this paper we investigated the absorption properties of homogeneous MIM structures. We derived and provided analytical formulas (equations (5) and (6)) based on the transfer matrix approach for determining the parameters of such a structure in order to achieve perfect absorption for a given wavelength. We verified the theoretical model with rigorous simulations using RCWA, showing also that the high absorption is preserved even for large angles of incidence and for both TE and TM incident polarizations. Finally, we used the MIM absorber results to design multilayered MIM structures with several perfect absorption bands. The highly efficient absorption characteristics of our structures can be potentially deployed for solar cells, optical filter elements, sensors, etc.

Acknowledgments

References

[1] Cui Y *et al* 2014 Plasmonic and metamaterial structures as electromagnetic absorbers (review article) *Laser Photon. Rev.* **8** 495

[2] Ra'di Y, Simovski C R and Tretyakov S A 2015 Thin perfect absorbers for electromagnetic waves: theory, design, and realizations *Phys. Rev. Appl.* **3** 037001

[3] Meng L *et al* 2013 Polarization-sensitive perfect absorbers at near-infrared wavelengths *Opt. Express* **21** A111–22

[4] Liao Y L and Zhao Y 2014 A wide-angle dual-band polarization-sensitive absorber with a multilayer grating *Mod. Phys. Lett.* B **28** 1450109

[5] Mattiucci N *et al* 2012 Tunable, narrow-band, all-metallic microwave absorber *Appl. Phys. Lett.* **101** 141115

[6] Chanda D *et al* 2011 Coupling of plasmonic and optical cavity modes in quasi-three-dimensional plasmonic crystals *Nat. Commun.* **2** 479

[7] Young C *et al* 2014 Multi-narrowband absorber based on subwavelength grating structure *Opt. Commun.* **311** 310

[8] Li Z *et al* 2014 Ultranarrow band absorbers based on surface lattice resonances in nanostructured metal surfaces *ACS Nano.* **8** 8242

[9] Hao J, Zhou L and Qiu M 2011 Nearly total absorption of light and heat generation by plasmonic metamaterials *Phys. Rev.* B **83** 165107

[10] Liu N *et al* 2010 Infrared perfect absorber and its application as plasmonic sensor *Nano Lett.* **10** 2342

[11] Hibbins A P *et al* 2006 Resonant absorption of electromagnetic fields by surface plasmons buried in a multilayered plasmonic nanostructure *Phys. Rev.* B **74** 073408

[12] Teperik T V *et al* 2008 Omnidirectional absorption in nanostructured metal surfaces *Nat. Photon.* **2** 299

[13] Spirkl W and Ries H 1985 Solar thermophotovoltaics: an assessment *J. Appl. Phys.* **57** 4409

[14] Aydin K *et al* 2011 Broadband polarization-independent resonant light absorption using ultrathin plasmonic super absorbers *Nat. Commun.* **2** 517

[15] Yan M 2013 Metal–insulator–metal light absorber: a continuous structure *J. Opt.* **15** 025006

[16] Li Z *et al* 2015 Large-area, lithography-free super absorbers and color filters at visible frequencies using ultrathin metallic films *ACS Photonics* **2** 183

[17] Bouchon P *et al* 2012 Wideband omnidirectional infrared absorber with patchwork of plasmonic nanoantennas *Opt. Lett.* **7** 1038

[18] Gokhale V J *et al* 2014 Subwavelength plasmonic absorbers for spectrally selective resonant infrared detectors *IEEE Sensors* 982

[19] Jung Y U *et al* 2014 Dual-band photon sorting plasmonic MIM metamaterial sensor *Proc. SPIE* **9070** 90702X

[20] Chen Y *et al* 2014 Metal–insulator–metal plasmonic absorbers: influence of lattice *Opt. Express* **22** 30807

[21] Moharam M G and Gaylord T K 1981 Rigorous coupled-wave analysis of planar-grating diffraction *J. Opt. Soc. Am.* **71** 811

[22] Hubarevich A *et al* 2015 Ultra-thin broadband nanostructured insulator-metal–insulator–metal plasmonic light absorber *Opt. Express* **23** 9753

[23] Markoš P and Soukoulis C M 2008 *Wave Propagation: from Electrons to Photonic Crystals and Left-Handed Materials* (Princeton, NJ: Princeton University Press)

[24] Palik E D (ed)1985 *Handbook of Optical Constants of Solids* (New York: Academic)

[25] Ding K *et al* 2011 *Solar Energy Materials and Solar Cells* **95** 3318